Computer Methods in Applied Mechanics and Engineering 110 (1993) 157-169 North-Holland

Thermal convection in vertical cylinders. A method based on potentials of velocity

F. Marqués, M. Net, J.M. Massaguer and I. Mercader

Departament de Física Aplicada, Universitat Politècnica de Catalunya, 08034 Barcelona, Spain.

Received 16 November 1992
Revised manuscript received 7 March 1993

Any solenoidal vector field can be written in terms of two scalar fields. Solving the Naviers-Stokes equation for these two so-called potentials is a widely used method, though difficulties have been reported in using this method to describe non-cartesian confined flows, in particular cylindrical geometries. Difficulties arise because the potentials are coupled at the boundaries but also because of possible numerical instabilities associated with the high order of the equations. This paper shows how all these difficulties can be circumvented: firstly by properly deriving the required boundary conditions, but also through an adequate discretization, which is the final requirement. The use of spectral methods together with a reduction of order for the axisymmetric modes is sufficient for this purpose. In this paper, as a test, a velocity potentials method is used to solve the stability problem for the onset of convection in a fluid confined in a cylindrical container.

1 Introduction

Closed containers provide controlled boundary conditions in fluid flows, in contrast to open flows where the open sections of the delimiting pipes or channels may provide a source of unwanted noise. This effect, plus the presence of convective instabilities, i.e. instabilities growing in a Lagrangian frame of reference, may influence the structure of a turbulent flow, so it has been claimed that closed containers with controlled energy sources may provide a better experimental setting for turbulence [1].

In closed containers, in incompressible fluids the pressure field happens to be a hidden variable, so it is a quite natural and widespread practice to project the master equations into the space of divergence free velocity fields to eliminate pressure from the equations. Explicit use of the pressure, say a formulation in terms of the primitive variables, requires a specific technique to handle first order derivatives in a closed domain. Thus, properly solving the equations for the pressure at the boundaries becomes an awkward problem. This becomes a major problem if boundaries, especially lateral ones, are expected to control the dynamics of the flow, as seems to be the case for thermal convection in small and intermediate aspect ratio containers.

Writing the solenoidal velocity field in terms of two scalar potentials could be a better choice. Unfortunately, however, pressure elimination raises the order of the equations, and additional boundary conditions may be required [2]. Technical difficulties in handling boundary conditions for non-Cartesian geometries, and the high order of the resulting equations have discouraged many researchers, thus increasing the popularity of the primitive variables methods.

Our main goal is to show that neither the increased order of the differential equations nor the coupling of the boundary conditions diminishes the power of the method. We do so by applying this technique to the problem of convection in cylindrical geometry. This geometry is acknowledged

* *Correspondence to:* Dr. Francisco Marqués, UPC, Departament de Física Aplicada, Jorge Girona Salgado, 08034 Barcelona, Spain.

to produce awkward technical problems if velocity potentials are used, and some authors prefer to bypass difficulties by introducing ad hoc boundary conditions such as zero tangential vorticity on the side wall [3]. These artificial boundary conditions yield qualitative deviations with respect to the stress-free boundary conditions [4]. Marcus [5], for instance, encourages the use of primitive variable formulations. He derived an improved technique by using a variant of the so-called influence matrix method developed by Kleiser and Schumann [6] (see also [7] for a review). However, Marcus' paper warns about the sensitivity of the results with respect to artificial pressure boundary conditions. We show in this paper that velocity potential methods, if carefully designed, are powerful and safe.

The velocity potential methods have often been used in Cartesian [8–10] and spherical geometries [11] for modeling thermal convection, and the number of choices for the potentials that can be found in the literature is significantly large. But there are certain geometries where the variables couple at the boundaries and, as a result, some numerical techniques become useless, or simply give rise to unwanted instabilities; for instance, the Galerkin method is useless if variables are coupled through boundary conditions.

The linear problem for the onset of thermal convection in a cylindrical container has been used as a test, as it has been solved in the past for a number of different boundary conditions. For instance, in the axisymmetric case with stress-free boundary conditions both at lateral walls and lids [12–14]; also for stress-free top and bottom lids but a rigid lateral wall [15,16]. More recently, both the non-axisymmetric case with free boundary conditions everywhere, and the ad hoc case of a zero vertical vorticity wall with free top and bottom boundary conditions have also been solved [4]. The case of rigid boundary conditions everywhere can be found in [17,18] where a formulation based on a vector potential for the velocity field was used. Sabri [19] derived an integral method with a large convergence rate, which unfortunately is only feasible for a restricted class of boundary conditions.

In the present paper we examine the case of convection in a cylinder with a rigid side wall and either free or rigid top and bottom lids. In order to describe the velocity field, we have chosen a representation in terms of poloidal and toroidal potentials. For the temperature, both the conducting and the insulating case will be examined. For the numerical technique, emphasis is laid on pseudospectral methods, and both tau and collocation methods will be used and compared. Section 2 is devoted to the mathematical formulation of the problem. In Section 3 the linear stability of the conductive basic state is examined using two different spectral methods. In Section 4 the obtained results are discussed and compared with previously published work. Finally, in Section 5, we give some conclusions.

2 The velocity potentials method

Thermal convection will be studied in a cylindrical domain bounded at top and bottom by two horizontal plates at a vertical distance L and a vertical cylindrical surface of radius a as a lateral wall. A vertical temperature gradient is imposed by differentially heating the bottom (temperature $\theta = \theta_0$) and top ($\theta = \theta_0 - \Delta\theta$). We assume a Boussinesq fluid whose motion is governed by the Navier-Stokes and energy equations. The velocity field $\mathbf{v}$ is then incompressible.

$$\nabla \cdot \mathbf{v} = 0, \tag{2.1a}$$
$$\sigma^{-1}(\partial_t + \mathbf{v} \cdot \nabla)\mathbf{v} = -\nabla p + RT\mathbf{e}_z + \Delta \mathrm{v}, \tag{2.1b}$$
$$(\partial_t + \mathbf{v} \cdot \nabla)T = \Delta T + v_z. \tag{2.1c}$$

We have adimensionalized the equations using L, L^2/κ, κ^2/L^2, $\Delta\theta$ for space, time, pressure (in fact p/ρ, including the gravity potential term) and temperature, respectively, where κ is the thermal diffusivity. The nondimensional parameters are the aspect ratio $A = a/L$, the Rayleigh number $R = \alpha\,\delta\theta\,gL^3/\nu\kappa$ and the Prandtl number $\sigma = \nu/\kappa$. ?alpha is the coefficient of thermal expansion, ν the kinematic viscosity, g the acceleration of gravity, $\mathbf{e}_z$ the unit vertical vector and T the temperature excess from the conductive state, $T = (\theta - \theta_0)/\Delta\theta + z$. The corresponding boundary conditions in cylindrical coordinates are

$$\left.\begin{array}{l} v_r = v_\theta = v_z = 0 \\ T = 0 \text{ (conducting)}, \ \partial_r T = 0 \text{ (insulating)} \end{array}\right\} \quad \text{on } r = A, \tag{2.2a}$$

$$\left.\begin{array}{ll} v_z = \partial_z v_r = \partial_z v_\theta = T = 0 & \text{(free lids)} \\ v_r = v_\theta = v_z = T = 0 & \text{(rigid lids)} \end{array}\right\} \quad \text{on } z = 0, 1. \tag{2.2b}$$

In order to eliminate the pressure by using the incompressibility condition, we have assumed that

$$\mathbf{v} = \nabla \times \nabla \times (\phi \mathbf{e}_z) + \nabla \times (\psi \mathbf{e}_z) \tag{2.3}$$

and replaced the Navier-Stokes equation (2.1b) with the z-components of their curl and double-curl. As shown in [2], equivalence between both formulations may require additional boundary conditions. We shall show below that in the cylindrical case only one boundary condition is to be added. Conditions for the existence of potentials ϕ and ψ in an arbitrary domain can be found in the aforementioned paper.

PROPOSITION. Equations (2.1), (2.2) are equivalent to

$$(\sigma^{-1}\partial_t - \Delta)\Delta_h \psi = \mathbf{e}_z \cdot (\nabla \times \mathbf{b}), \tag{2.4a}$$
$$(\sigma^{-1}\partial_t - \Delta)\Delta\Delta_h \phi = -R\Delta_h T - \mathbf{e}_z \cdot (\nabla \times \nabla \times \mathbf{b}), \tag{2.4b}$$
$$(\partial_t - \Delta)T = -\Delta_h \phi - \mathbf{v} \cdot \nabla T, \tag{2.4c}$$

where $\Delta_h = r^{-1}\partial_r(r\partial_r) + r^{-2}\partial^2_{\theta\theta}$, $\mathbf{b} = \sigma^{-1}(\mathbf{v} \cdot \nabla \mathbf{v})$. *Boundary conditions are*

$$\phi = \partial_r \phi = \Delta_h \phi = 0, \tag{2.5a}$$
$$\frac{1}{r}\partial_\theta \psi + \partial^2_{rz}\phi = 0, \ T = 0 \ (or\ \partial_r T = 0), \tag{2.5b}$$
$$R\partial_\theta T + r\partial^2_{rz}\Delta_h \psi - \partial_\theta \Delta\Delta_h \phi = 0 \tag{2.5c}$$

on $r = A$, *together with*

$$\left.\begin{array}{ll} \phi = \partial^2_{zz}\phi = \partial_z \psi = T = 0 & \textit{(free lids)} \\ \phi = \partial^2_z \phi = \psi = T = 0 & \textit{(rigid lids)} \end{array}\right\} \quad \textit{on } z = 0,\ 1. \tag{2.5d}$$

Equivalence means that if $\{\mathbf{v}, T\}$ *is a solution of (2.1), (2.2) then the corresponding potentials (2.3) satisfy (2.4), (2.5). And inversely if* $\{\psi, \phi, T\}$ *is a solution of (2.4), (2.5) the corresponding* $\{\mathbf{v}, T\}$ *obtained by using (2.3) satisfy (2.1), (2.2).*

PROOF. In order to prove the equivalence we shall proceed in several steps. For convenience, let us write (2.1b) as

$$\mathbf{N} = -\nabla p \tag{2.6}$$

where $\mathbf{N}$ includes every term but the pressure gradient. In a simply connected domain, as is the present case, (2.6) is equivalent to

$$\nabla \times \mathbf{N} = 0 \tag{2.7}$$

Therefore, we must only prove the equivalence between (2.7) and the following equations

$$\mathbf{e}_z \cdot (\nabla \times \mathbf{N}) = 0, \quad \mathbf{e}_z \cdot (\nabla \times \nabla \times \mathbf{N}) = 0, \tag{2.8a}$$

in the bulk of the fluid domain $\Omega = \{0 \le r \le A,\ 0 \le \theta \le 2\pi,\ 0 \le z \le 1\}$ together with

$$\mathbf{e}_r \cdot (\nabla \times \mathbf{N}) = 0, \tag{2.8b}$$

in the lateral boundary $\partial_L \Omega = \{r = A\}$. It must be noticed that (2.8a) is a compact form for (2.4a,b), as is (2.8b) for (2.5c).

The direct implication is immediate. To prove the converse we define $\mathbf{Q} \equiv \nabla \times \mathbf{N}$. Equation (2.8a-1) reads $Q_z = 0$ and equation (2.8a-2) implies that in every z horizontal circle D_z a function κ exists such that

$$Q_\theta = \frac{1}{r}\partial_\theta \kappa, \quad Q_r = \partial_r \kappa.$$

The solenoidal character of Q together with (2.8b) give the following problem

$$\Delta_h \kappa = 0 \ \text{ in } D_z, \quad \partial_n \kappa = 0 \ \text{ in } \partial_L \Omega|_{D_z}.$$

Thus, κ is the solution of the homogeneous Neumann problem in D_z and is therefore constant. As a consequence, $\mathbf{Q} = 0$, so proving the equivalence between (2.7) and (2.8). Equation (2.8b) is a boundary condition to be added to the original problem for consistency. It is required because the order of the system has been increased. Now, by using the equalities $\mathbf{e}_z \cdot \mathbf{v} = -\Delta_h \phi$, $\mathbf{e}_z \cdot (\nabla \times \mathbf{v}) = -\Delta_h \psi$, and $\mathbf{e}_z \cdot (\nabla \times \nabla \times \mathbf{v}) = \Delta \Delta_h \phi$, equations (2.4) can be obtained from (2.8a) and (2.1c), so proving the equivalence.

In order to integrate the system, six boundary conditions on rt=tA are required, and there are only five: four resulting from the boundary conditions on v and T (2.2a) and one from (2.8c). The sixth one comes from the freedom in choosing the gauge for the potentials. In order to decide the gauge it must be noticed that the solution of the homogeneous problem $\mathbf{v} \equiv 0$ is given by

$$\Delta_h \phi = 0, \quad \nabla_h \psi = -\mathbf{e}_z \times \nabla(\partial_z \phi),$$

where $\nabla_h = (\partial_r, r^{-1}\partial_\theta)$. Therefore, ϕ is determined up to a horizontal harmonic function, i.e. harmonic in r and θ but arbitrary in z. With regard to ψ, an arbitrary function of z can be added. We shall choose $\phi = 0$ at $r = A$. This condition and the boundary conditions (2.2a), (2.8b) written in terms of potentials give (2.5a,b,c). Conditions (2.5b) and (2.5c) couple the potentials and the temperature, but as we shall see below, this is not a serious difficulty when using spectral methods.

On the top and bottom plates (z=0, 1), only four boundary conditions are required to integrate (2.4), because Δ_h does not contain ∂_z. The free boundary conditions at the top and bottom, $v_z = 0$, $\partial_z v_r = 0$, $\partial_z v_\theta = 0$ (2.2b), written in terms of the potentials, give

$$\frac{1}{r}\partial^2_{\theta z}\psi + \partial^3_{rzz}\phi = 0, \quad \partial^2_{rz}\psi - \frac{1}{r}\partial^3_{\theta zz}\phi = 0, \quad \Delta_h \phi = 0. \tag{2.9}$$

The gauge freedom $\phi = 0$ at $r = A$ together with (2.9c) gives $\phi = 0$ at z=0, 1. It is easy to show that $\partial_z \psi = 0$ and $\partial^2_{xx}\phi = 0$ are equivalent to (2.9a) and (2.9b). The direct implication is trivial. To prove the converse we notice that (2.9b) implies $\partial_z \psi = \partial_\theta f$, $\partial^2_{xx}\phi = r\partial_r f$ for a prescribed function $f(r, \theta)$. By substituting these conditions into (2.9a) we obtain $\Delta_h f = 0$. But $\partial_r f = 1/r\, \partial^2_{rz}\phi = 0$ on $r = A$, because of (2.5a), so f is the solution of the homogeneous Neumann problem at z=0, 1. Then f is constant, thus giving $\partial_z \psi = 0$ and $\partial^2_{xx}\phi = 0$. Therefore, (2.5d) is fulfilled.

The rigid boundary conditions at top and bottom in terms of the potentials are

$$\frac{1}{r}\partial_\theta\psi + \partial^2_{rz}\phi = 0, \tag{2.10a}$$
$$\partial_r\psi - \frac{1}{r}\partial^2_{\theta z}\phi = 0, \tag{2.10b}$$
$$\Delta_h\phi = 0. \tag{2.10c}$$

Boundary conditions $\partial_z\phi = 0$ and $\psi = 0$ are equivalent to (2.10a) and (2.10b). The proof is exactly the same as in the preceding case , because (2.9a,b) is the z-derivative of (2.10a,b). And $\Delta_h\phi = 0$ on z=0, 1 together with the lateral wall boundary condition $\phi = 0$, means that $\phi = 0$ on z=0, 1, so we obtain (2.5e), and the proof is complete. □

In the axisymmetric case ($\partial_\theta = 0$) a reduction in the order of the equations is possible because (2.4a,b) are now total derivatives. In this case the order of the first two equations (2.4) is reduced to two and four, and the coupled boundary conditions (2.5b,c) are replaced by uncoupled ones. For more details see [2,20].

3 Linear stability of the conductive state

The conductive state is characterized by $\mathbf{v}^0 = 0$, i.e. $\phi^0 = \psi^0 = 0$, and $T^0 = 0$. The small perturbations ϕ', ψ' and T' can be Fourier expanded in θ as

$$\begin{aligned}\psi'(r,\theta,z,t) &= ie^{\lambda t}\sum_n \psi_n(r,z)e^{in\theta},\\ \phi'(r,\theta,z,t) &= e^{\lambda t}\sum_n \phi_n(r,z)e^{in\theta},\\ T'(r,\theta,z,t) &= e^{\lambda t}\sum_n T_n(r,z)e^{in\theta}.\end{aligned} \tag{3.1}$$

Thus, in the linearized version of (2.4), the equations for each index n are uncoupled.

3.1 The numerical method

As a preliminary step for solving the linear problem we have introduced the following set of auxiliary functions for every index n

$$\psi_1 = \Delta_h\psi, \quad \phi_1 = \Delta_h\phi, \quad \phi_2 = \Delta\phi_1, \tag{3.3}$$

where $\Delta_h = r^{-1}\partial_r(r\partial_r) - n^2/r^2$, $\Delta = \Delta_h + \partial^2_{zz}$, with the eigenvalue problem written as

$$\lambda/\sigma\,\psi_1 = \Delta\psi_1, \quad \lambda/\sigma\,\phi_2 = \Delta\phi_2 - R\Delta_h T, \quad \lambda T = \Delta T - \phi_1. \tag{3.4}$$

The boundary conditions (2.2a) at $r = A$ are

$$\phi = \phi_1 = \partial_r\psi = \partial^2_{rz}\phi - \frac{n}{A}\psi = 0, \quad T = 0 \text{ or } \partial_r T = 0, \quad n\phi_2 - A\partial^2_{rz}\psi_1 - nRT = 0, \tag{3.5}$$

and at z=0, 1 the boundary conditions are (2.5d). These conditions are equivalent to

$$\left.\begin{array}{ll}\phi = \partial^2_{zz}\phi = \partial_z\psi = T = 0 & \text{(free lids)}\\ \phi_1 = \partial_z\phi_1 = \psi = T = 0 & \text{(rigid lids)}\end{array}\right\} \quad \text{on } z = 0,\ 1. \tag{3.6}$$

The eigenvalue problem (3.3)–(3.6) has been defined in the radial interval $[0, A]$, although strictly speaking boundary conditions exist only at the points $r = A$. At the point $r = 0$, which is in fact an interior point for the two-dimensional domain, conditions concerning the regularity of the solution and their derivatives must be imposed. In fact, the boundary conditions imposed at $r = 0$ are crucial; if some of the boundary conditions at $r = 0$ are too restrictive, the critical Rayleigh number can be overestimated. So at $r = 0$ we shall impose the minimum number of boundary conditions that ensure regularity. We have taken as regularity conditions at $r = 0$

$$\phi = \phi_1 = \phi_2 = \psi = \psi_1 = T = 0. \tag{3.7}$$

In order to avoid difficulties associated with a formal singularity at $r = 0$, equations (3.3), (3.4) can be multiplied by r. By proceeding in this way, regularity conditions (3.7) need not be explicitly enforced. We have compared both methods and we got the same results.

Systems (3.3) and (3.4) together with boundary conditions (3.5), (3.6) and (3.7) define the exact eigenvalue problem for the non-axisymmetric case. The corresponding equations for the axisymmetric case were obtained in a similar way [20].

From (3.3) we can solve $\{\psi, \phi, \phi_1\}$ as functions of $\{\psi_1, \phi_2\}$ by sequentially inverting the three laplacians. Now, (3.4) reduces to a eigenvalue problem $AX = \lambda X$, with X being of dimension $3N$, with N being the number of unknowns for $\{\psi_1, \phi_2, T\}$.

In the present paper we have solved two different linear problems. First of all, the critical Rayleigh number for the onset of instability has been obtained as a function of the aspect ratio, by taking $\lambda = 0$ in (3.4), as the problem is selfadjoint, and λ is real. Next, the full spectra of eigenvalues λ has been computed for Rayleigh numbers near criticality, so as to obtain information on the efficiency of the method.

Both problems have been solved by tau and collocation methods with the potentials expanded in Chebyshev polynomials for the r-coordinate. As boundary conditions at z=0, 1 for the stress-free and rigid lid cases are different, for the z-coordinate we have used a trigonometrical-Galerkin expansion in the free case

$$X^i(\xi, z) = \sum_{m=0}^{M} \sum_{l=0}^{L} a^i_{l,m} T_l(\xi) \sin m\pi z, \tag{3.8a}$$

$$Y^i(\xi, z) = \sum_{m=0}^{M} \sum_{l=0}^{L} b^i_{l,m} T_l(\xi) \cos m\pi z, \tag{3.8b}$$

where $X = \{\phi, \phi_1, \phi_2, T\}$ and $Y = \{\psi, \psi_1\}$, and a series expansion in Chebyshev polynomials for the rigid case

$$X^i(\xi, \zeta) = \sum_{m=0}^{M} \sum_{l=0}^{L} a^i_{l,m} T_l(\xi) T_m(\zeta), \tag{3.9}$$

with $X = \{\psi, \psi_1, \phi, \phi_1, \phi_2, T\}$, $\xi = 2r/A - 1$ and $\zeta = 2z - 1$. Notice that in the stress-free case, the linear equations are uncoupled for both indices n and m (azimuthal and vertical dependence) but not in the rigid one.

We have taken the same number of modes (M, L) for every unknown because our leitmotif is pseudospectral non-linear calculations. In the tau method, the unknowns are the coefficients $a^i_{l,m}$. In the Chebyshev collocation method the unknowns are the values of the potentials and temperature at the Gauss-Lobato grid points $\xi_l = \cos \pi l/L$ $(l = 0, \ldots, L)$ and $\zeta = \cos \pi m/M$ $(m = 0, \ldots, M)$. Once boundary conditions are imposed, the number of unknowns can be explicitly reduced. We shall call number of degrees of freedom for each variable, the number of unknowns remaining once these boundary condition relationships have been used to reduce the number of unknowns.

Although (3.3), (3.4) have been formally written in terms of laplacian operators, it is not possible to associate one single boundary condition to each one of these functions, and this is a well known source of instabilities. The best known examples of such instabilities come from biharmonic operators with boundary conditions on the unknown function and its first derivative [21]. In a previous paper [20] we have introduced some numerical techniques to avoid such instabilities. In this paper we have used two closely similar methods.

The first method solves, sequentially, (3.3c, b, a) with boundary conditions $\phi_1 = 0$, $\phi = 0$, $\psi = An^{-1}\partial^2_{rz}\phi$ on $r = A$. Then, it solves (3.4) but, so as to avoid spurious eigenvalues, boundary condition $\partial_r\psi = 0$ is to be changed into a condition for ψ_1. In order to do so, we shall write on the boundary $\psi_1 = \Delta\psi$ by using $\partial_r\psi = 0$ as in [22]. Thus, we shall have L degrees of freedom in r for every variable. A similar procedure can be used for $\partial_z\phi_1 = 0$ at z=0, 1.

The second method solves system (3.3) as before, but using at $r = A$ the two boundary conditions for ψ, $\psi = An^{-1}\partial^2_{rz}\phi$, $\partial_r\psi = 0$. Thus, the number of degrees of freedom for ψ and ψ_1 in the radial direction is $L - 1$. Thus different variables may have different number of degrees of freedom. As boundary conditions for (3.4) we shall also use the equation $\psi_1 j = \Delta\psi$ in the two points closest to $r = A$. A similar procedure can be used for $\partial_z\phi_1 = 0$ at z=0, 1.

It is also possible to use a third method inspired in the implicit method of Canuto [23,24]. Accordingly, an auxiliary variable defined by $\psi' = \partial_r\psi$ is introduced, with ψ' expanded as in (3.8b) or (3.9). The definition $\psi' = \partial_r\psi$ is explicitly enforced at every interior point, and (3.3a) is evaluated by using the relations $\psi' = \partial_r\psi$ and $\partial_r\psi' = \partial^2_{rr}\psi$ at every point including the boundaries, thus allowing us to obtain ψ_1 at $r = A$. In the rigid lids case the value of ϕ_2 at z=0, 1 is also required. Again an auxiliary variable $\phi_1^* = \partial_z\phi_1$, expanded as in (3.9) is introduced. But this is a less efficient method for it is more time consuming and requires a larger memory size.

4 Numerical results

The present paper addresses the questions of feasibility and efficiency of a potentials velocity method. Proper implementation of the boundary conditions is certainly the cornerstone, and we have therefore computed and carefully examined results for the most frequently used boundaries. All

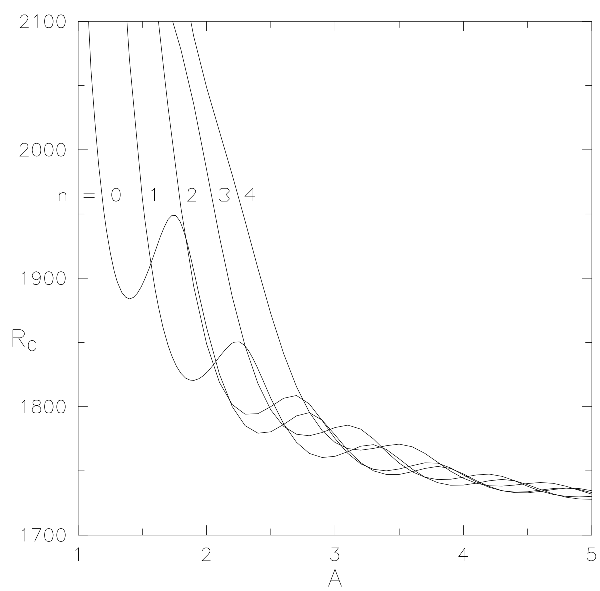

Fig. 1. Critical Raleigh numbers R_c corresponding to the first five azimuthal modes ($n = 0, \ldots, 4$) in the insulating lateral wall case, for rigid lids. A is the cylinder's aspect ratio.

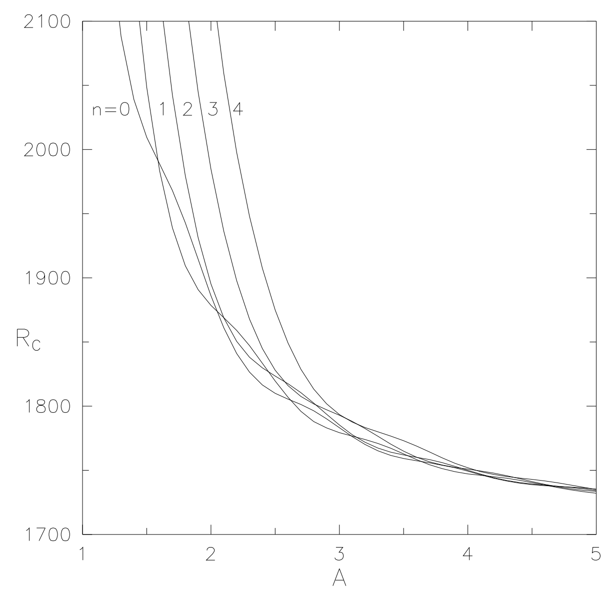

Fig. 2. Critical Raleigh numbers R_c corresponding to the first five azimuthal modes in the perfectly conducting lateral wall case, for rigid lids.

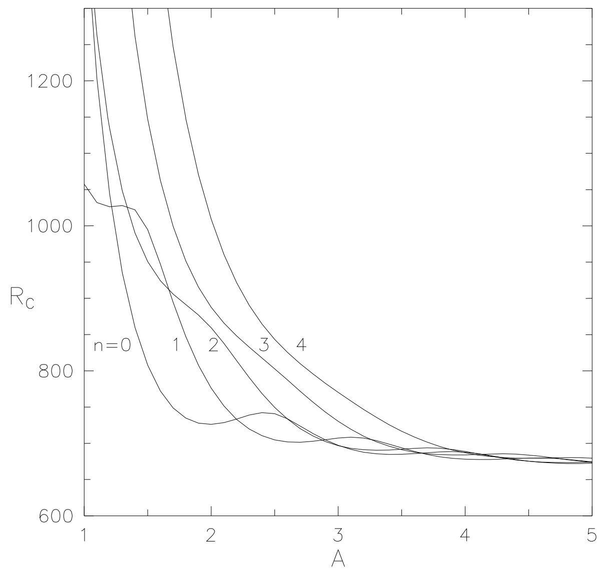

Fig. 3. Critical Raleigh numbers R_c corresponding to the first five azimuthal modes in the insulating lateral wall case, for stress-free lids.

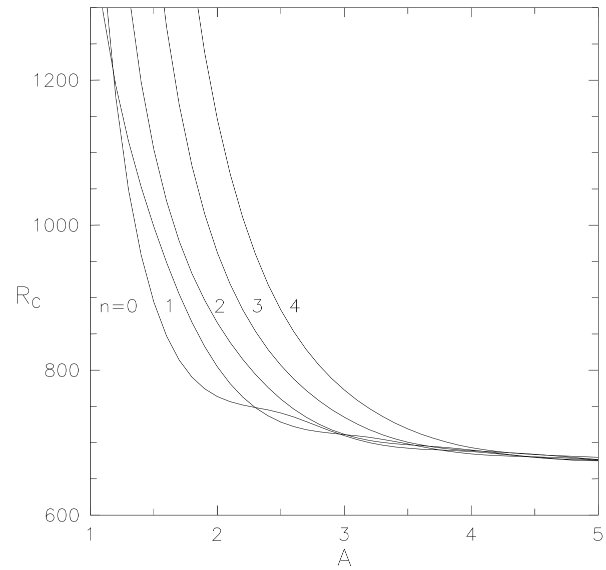

Fig. 4. Critical Raleigh numbers R_c corresponding to the first five azimuthal modes in the perfectly conducting lateral wall case, for stress-free lids.

combination of stress-free or rigid top and bottom lids with thermal or insulating boundaries have been considered. We display in figures 1 to 4 the marginal stability curves as a function of the aspect ratio for every one of these combinations as a function of the azimuthal number n. The rigid boundary results had been computed previously by other authors and using different techniques [18], [19].

For aspect ratio containers smaller than 0.1 the numerical method can produce ill-conditioned matrices. Therefore, in order to compute the marginal stability curves for small A-values, a perturbative analysis is required. Proper fitting between these analytically computed marginal states and the ones numerically computed has been taken as an additional check for consistency. To do so we have assumed the expansion $RA^4 = \mu_0 + \mu_1 A^2 + \ldots$ and then computed μ_k order by order. In the free lids case the computation is straightforward. A two terms expansion gives the critical Rayleigh number exact within 1% in the range $0 \leq A \leq 0.5$, except for the zero-mode, showing such an error bar within a smaller range $0 \leq A \leq 0.15$. The values of μ_0, μ_1 for the first azimuthal modes are listed in Table 1, and details of the method can be found in the Appendix A.

In the rigid case the problem is slightly more complicated, as the boundary conditions preclude the existence of a unique orthonormal basis to expand every dependent variable $\{\psi, \phi, T\}$. However, the leading order equations (A.3) obtained for the temperature and for the critical Rayleigh number

Table 1
Coefficients μ_0, μ_1 in the perturbation series of the critical Rayleigh number, for the first azimuthal modes; μ_0 takes the same value for free and rigid lids; μ_1 is given only for the free case

	Conducting		Insulating	
n	μ_0	μ_1	μ_0	μ_1
0	452.00	1492.27	452.00	878.65
1	215.56	513.78	67.96	306.67
2	695.62	899.32	328.89	631.64
3	1657.01	1362.71	942.51	1041.92
4	3315.90	1901.20	2102.21	1531.58
5	5920.06	2512.93	4033.50	2096.89

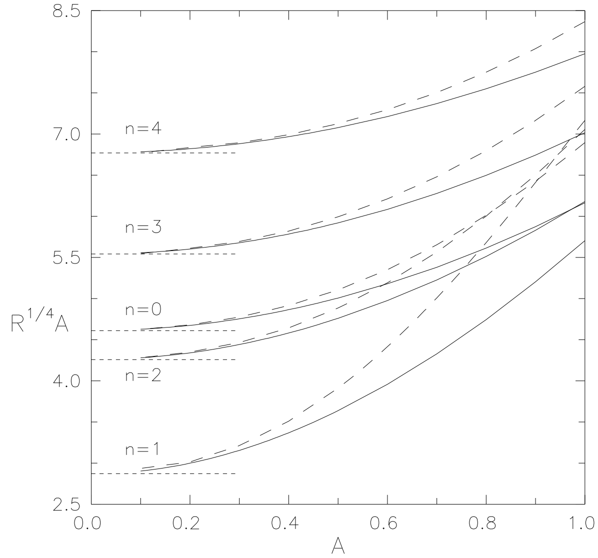

Fig. 5. Comparison between computed and asymptotic values (point lines) of the critical Rayleigh numbers for the first five azimuthal modes in the insulating case. Solid lines correspond to the free lids case, and dashed lines to the rigid one.

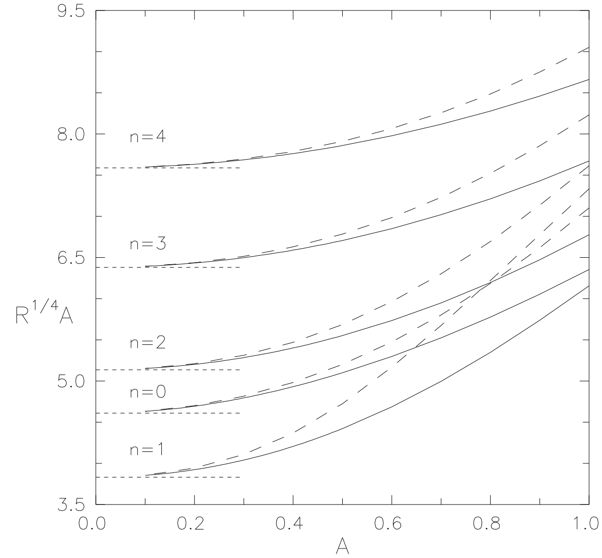

Fig. 6. Comparison between computed and asymptotic values (point lines) of the critical Rayleigh numbers for the first five azimuthal modes in the conducting case. Solid lines correspond to the free lids case, and dashed lines to the rigid one.

in the rigid case are the same as those found for the free case described above. In Figures 5 and 6 the asymptotic values for the transition curves have been plotted together with the ones numerically computed. The fit of both curves is excellent, but the Figures show in addition the convergence of marginal curves for the free and rigid lids cases, as expected from the asymptotics.

The numerical results show that the only remarkable difference between the rigid and free lids cases for small A is the presence of top and bottom boundary layers for the former but not for the latter. Resolving these boundary layers numerically increases substantially the required effort, as will be shown below, and is the cause of the numerical difficulties involved in computing the flow for small A values. In order to give a graphic illustration of the differences between both cases we have shown in Figure 7 the isotachs for the radial velocity and the isolines for the vertical vorticity, both for a small aspect ratio, $A = 0.1$, cylinder. The top and bottom boundary layers are fairly obvious in the rigid case but non-existent for the free one. The lack of lateral boundary layers in both cases must be noted. In figure 7d we have displayed the constant vertical vorticity lines for the rigid lids case. For this particular example, we have explicitly imposed as boundary condition $\partial_r \psi = 0$, because any other procedure to impose boundary condition on ψ (see Section 3) produced rough isovorticity lines near the boundaries. Thus, in any problem where shear at the lateral boundary may play a role, tricks to bypass the boundary condition $\partial_r \psi = 0$ are to be avoided. The previous discussion shows that a velocity potentials method coupled with a pseudo-spectral technique, either collocation or tau, provides a convenient tool for solving the convection equations in a cylindrical domain. There is still a question about efficiency. The number of modes needed to obtain the desired accuracy (four figures) is 64 (8 in both radial and vertical directions) for intermediate A ($A \simeq 1$). As can be expected, the number of vertical modes increases with decreasing A, and the number of radial modes increases with increasing A. In Figure 8 we have displayed the critical Rayleigh number as a function of the number of modes for tau and collocation methods in order to compare their relative efficiency. We have chosen the rigid case, for this is the one that couples the radial and vertical dependence of the variables, and therefore is the most severe test. We display results for a slender cylinder, $A = 0.5$, and for $L = 12$ radial modes. Both methods give similar results. In evaluating the efficiency, the reader must be aware that the results displayed in Figure 8 show errors much smaller than in most published papers, where error bars of a few percentage points are frequent.

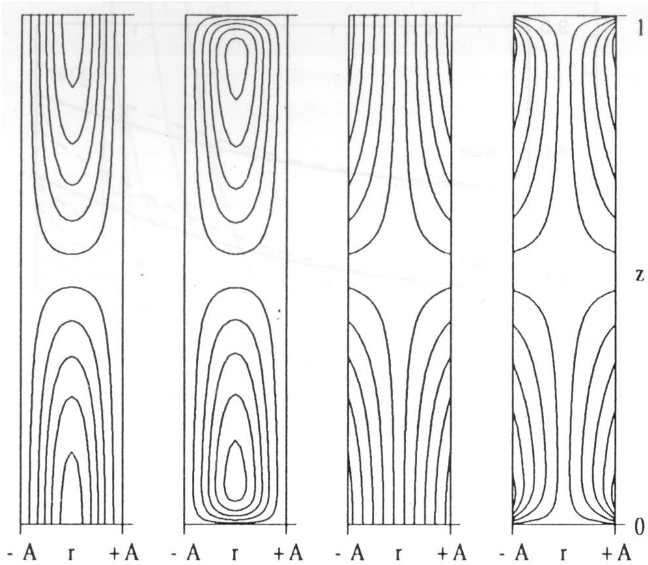

Fig. 7. (a) Isotachs for the radial velocity, free lids. (b) Isotachs for theradial velocity, rigid lids. (c), (d) Isolines for the vertical vorticity (free and rigid cases). Aspect ratio, $A = 0.1$. The top and bottom boundary layers are fairly obvious in the rigid case but non-existent for the free one.

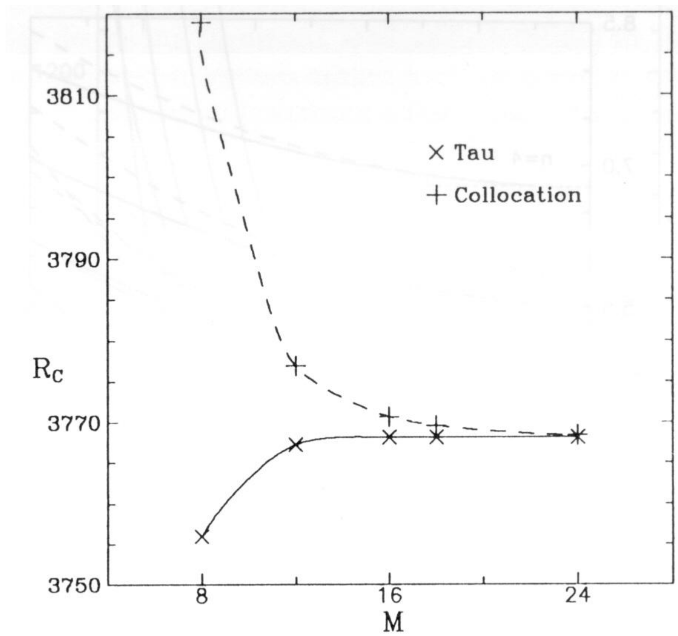

Fig. 8. Critical Rayleigh number as a function of the number of vertical modes for tau and collocation methods. Rigid lids case, $A = 0.5$. The number of radial modes is $L = 12$.

Finally we have computed the growth rates λ near the onset of instability, as it is well known that some spectral techniques may give spurious eigenvalues in the time spectrum for some treatments of the boundary conditions [21]. We have found that the full spectrum is well behaved, with numerical values converging at a convenient rate. For the free lids case with $N = 32$ the eigenvalue with maximum absolute value is $\lambda = -2.9 \times 10^6$ and the estimated error is smaller than two percent; see [20] for a detailed account. As an additional result of relevance for the non-linear case, it is worth mentioning that the eigenvalues in the rigid case increase in absolute value with the number of modes L, M with a law that can be estimated as $\lambda \simeq -c \times L^4 \times M^2$, compared with the standard $\lambda \sim N^2$ for a laplacian operator. c depends on the aspect ratio A , its value is 0.03 for $A = 0.5$ and it is smaller the larger the aspect ratio. This result is consistent with the coupling between the vertical velocity and vorticity equations through the lateral boundaries. In other formulations, say a primitive variables formulation, the coupling is provided by the pressure. Only a reduction in the number of modes can result in a reduction of the largest negative eigenvalue, and this is an important remark on the efficiency expected for the non-linear problem, where λ controls the step size if explicit, or even semiimplicit, time integrations are used.

5 Discussion and conclusions

In the present paper it has been shown that the velocity potentials method is a useful tool even in cylindrical geometries. Besides comparison with results of other authors, the total agreement between the numerical results and the perturbative expansion for small radius is completely satisfactory. By using spectral methods, any possible difficulty arising from the coupled boundary conditions has been avoided. Furthermore, spurious modes have also been avoided by using a method based on the explicit determination of the boundary conditions for high order derivatives, together with a reduction of order for the axisymmetric modes.

The velocity potentials method has been used to solve the stability problem of thermal convection in a cylindrical container with free and rigid top and bottom lids and a rigid side wall. Critical

Table 2
Comparison of the present results (column a) with those of [18] (column b). The b values where obtained from Figs. 5 and 6 of [18] and the interpolation is believed to be accurate within 2%.

	$R_{\rm crit}$ conducting		$R_{\rm crit}$ insulating	
n	a	b	a	b
0	1.306E+5	1.32E+5	1.273E+5	1.31E+5
1	6.660E+4	6.66E+4	2.378E+4	2.37E+4
2	1.954E+4	2.00E+5	9.608E+4	9.89E+4

Rayleigh numbers have been obtained for small and intermediate aspect ratios, $A = 0 - -5$, with the limit of small A being derived from a perturbative analysis. The results for the rigid lids case are coincident with those in Buell and Catton [18], and the critical Rayleigh numbers in both free and rigid lids have been found to be coincident in the limit $At \to 0$, suggesting that in that limit thermal convection is almost independent of top and bottom boundary conditions. It is also worth mentioning the existence of multicritical transition points, for they might produce very complicated dynamics in their neighborhood. Figures 1, 2, 3 and 4 show a lot of such transition points for different values of n (bicritical points). For some of these points, even a third mode appears very close to them, so increasing the complexity of the convection pattern.

We also have checked on the efficiency and stability properties of the different methods used to treat the boundary conditions. The results are clearly in favor of the second method, consisting on imposing all boundary conditions as such. Also, tau and collocation techniques give similar results, although tau method needs a smaller number of modes than collocation does. However we must notice that the tau method has received a special treatment so as to avoid the singularity at $r = 0$, i.e. we have multiplied the equations by r^2, so allowing an analytical development for the linear terms. Therefore we may warn the reader that the extension of the method to the nonlinear case [25] may not preserve the preference for the tau method. Finally, in order to stress the relevance of the techniques discussed before, we shall recall the efficiency of pseudospectral against Galerkin methods, with the later requiring N^2 operations for every direction against $N \log N$ in the former. Thus, these pseudospectral techniques have been proved more efficient than other Galerkin based methods, used in the literature, even if the number of modes required there is smaller.

Acknowledgement

This work was supported by the Dirección General de Investigación Científica y Técnica (DGICYT), under grants PS87/0107 and PB91/0595.

Appendix A. Asymptotic expansion for small A.

The parameter A defines the r-domain $[0, A]$, so it is only present through the boundary conditions at $r = A$ (3.5a,c). The limit $A = 0$ is formally singular, but singularity is avoidable. The change of variables $r = Ax$ in (3.4) gives

$$\Delta\Delta_h\psi = 0, \quad \Delta\Delta\Delta_h\phi - \mu\Delta_h T = 0, \quad \Delta T - \Delta_h\phi = 0, \tag{A.1}$$

where $\Delta_h = x^{-1}\partial_x(x\partial_x) - n^2/x^2$, $\Delta = \Delta_h + A^2\partial^2_{zz}$, $\mu = RA^4$ and $x \in [0, 1]$. Boundary conditions (3.5), (3.6) are modified in a similar way.

A.1 Free lids case

From (3.11) we can write

$$\begin{aligned}&\psi(x,\theta,z)=\psi(x)e^{in\theta}\cos m\pi z, \quad \phi(x,\theta,z)=\phi(x)e^{in\theta}\sin m\pi z,\\&T(x,\theta,z)=T(x)e^{in\theta}\sin m\pi z,\end{aligned}\tag{A.2}$$

Now, $\Delta=\Delta_h-m^2\pi^2A^2$, and the differential system (A.1) becomes regular for $A=0$. So we can expand ψ, ϕ, T and m as power series in A^2, say $T=A^2T_0+A^4T_1$. By solving (A.1) order by order a hierarchy of linear differential systems is obtained. At leading order

$$\begin{aligned}&(\Delta_h^2-\mu_0)\Delta_h T_0=0,\\&\Delta_h T_0=\mu_0 T_0-\Delta_h^2 T_0=0, \quad T_0 \text{ (or } \partial_x T_0)=0, \quad \text{on } x=1,\end{aligned}\tag{A.3}$$

with the whole system written in terms of T_0. This eigenvalue problem can be easily solved numerically. The minimum eigenvalue μ_0 and the corresponding eigenfunction T_0 can be obtained for each n. In addition ψ_0 and ϕ_0 can be found as solutions of the non-homogeneous problem

$$\begin{aligned}&\Delta_h^2\psi_0=0, \quad \Delta_h\phi_0=\Delta_h T_0,\\&\phi_0=\partial_x\psi_0=m\pi\partial_x\phi_0-n\psi_0=0 \text{ on } x=1,\end{aligned}\tag{A.4}$$

The technique can be pushed at higher orders in the usual way. Calculations are straightforward. As an example, μ_1 is given by

$$\mu_1=\frac{\left[\dfrac{m\pi}{n}(\partial_x T_0^*)\partial_x\Delta_h\psi_0-m^2\pi^2T_0\partial_x\Delta_h T_0^*\right]_{x=1}-3m^2\pi^2\displaystyle\int_0^1 xT_0^*\Delta_h^2T_0\,dx}{[T_0\partial_x T_0^*]_{x=1}+\displaystyle\int_0^1 xT_0^*\Delta_h T_0\,dx},\tag{A.5}$$

where T_0^* is the solution of the adjoint problem to (A.3). The m value corresponding to the critical Raleigh number has been found to be $m=1$ in all cases examined.

A.2 Rigid lids case

In this case the ϕ potential cannot be expanded as (A.2) because of the boundary conditions (2.5e). It is necessary to use the C_m and S_m functions introduced by Harris and Reid [26,27]. We assume

$$\begin{aligned}&\psi(x,\theta,z)=e^{in\theta}\sum_{m=1}^{\infty}\psi_m(x)\sin m\pi z,\\&\phi(x,\theta,z)=e^{in\theta}\sum_{m=1}^{\infty}(\phi_m(x)C_m(z)+\tilde{\phi}_m(x)S_m(z)),\\&T(x,\theta,z)=e^{in\theta}\sum_{m=1}^{\infty}T_m(x)\sin m\pi z,\end{aligned}\tag{A.6}$$

where the summation over m cannot be avoided. Substitution of (A.6) in (A.1) and subsequent development in A^2 gives a cumbersome set of coupled differential systems. But at zero order the equations for the temperature and the critical Raleigh number are still (A.3), so these magnitudes are the same in both the free and rigid lid cases. The corresponding equations for the velocity potentials ψ and ϕ are more involved than (A.4). They can be written as

$$\Delta_h\phi_{m,0}=\sum_{s=0}^{\infty}C_{s,m}\Delta_h T_{s,0}, \quad \Delta_h\tilde{\phi}_{m,0}=\sum_{s=0}^{\infty}S_{s,m}\Delta_h T_{s,0},\tag{A.7}$$

with boundary conditions $\phi_{m,0} = \tilde{\phi}_{m,0} = 0$ on $x = 1$,

$$\Delta_h^2 \psi_{m,0} = 0, \tag{A.8}$$

$$\partial_x \psi_{m,0} = 0, \ \psi_{m,0} = \frac{2}{n} \sum_{s=1}^{\infty} (C'_{s,m}\phi_{s,0} + S'_{s,m}\tilde{\phi}_{s,0}) \text{ on } x = 1, \tag{A.9}$$

where $\{C_{s,m},\ S_{s,m},\ C'_{s,m},\ S'_{s,m}\}$ are scalar products of the z-functions involved in the expansions, and $T_{s,0}$ are solutions of (A.3) differing only in a constant factor; these factors are determined at next order in A^2. But going to first order means solving a countable set of systems (A.7), (A.8). So in this case a direct numerical calculation from (A.1) is the only practical way to proceed. Solving higher order systems is of no relevance in the present context, but stressing the coincidence of both rigid and free systems at leading order helps us to understand why the non-separability of the rigid case does not pollute the numerical methods used.

References

[1] B. Castaing, G. Gunaratne, F.L. Heslot, L. Kadanoff, A. Libchaber, S. Thomae, X.Z. Wu, S. Zaleski, and G. Zanetti, J. Fluid Mech. 204 (1989).

[2] F. Marques, Phys. of Fluids A 2 (1990) 729–737.

[3] S. Rosenblat, J. Fluid Mech. 122 (1982) 395–410.

[4] C.A. Jones and D.R. Moore, Geophys. Astrophys. Fluid Dynamics 11, (1979) 245–270.

[5] P.S. Marcus, J. Fluid Mech. 146 (1984) 45.

[6] L. Kleiser and U. Schumann, in: E.H. Hirschel, ed., Proc. 3rd GAMM on Numerical Methods in Fluid Mechanics (Vieweg, Braunschweig, 1980) 165.

[7] L.S. Tuckerman, J. Comput. Phys. 80 (1989) 403-441.

[8] F.H. Busse, Rep. Prog. Phys. 41 (1978) 1929.

[9] J.M. Massaguer and I. Mercader, J. Fluid Mech. 189 (1988) 367.

[10] M. Nagata, J. Fluid Mech. 169 (1986) 229.

[11] P.S. Marcus, Astrophys. J. 231 (1979) 176.

[12] A. Pellew and R.V. Southwell, Proc. R. Soc. 176A (1940) 312–343.

[13] J. Zierep, Beitr. Phys. Atmos. 36 (1963) 70–76.

[14] S. Ostrach and D. Pneuli, J. Heat Transfer 85 (1963) 1346–1354.

[15] I. Catton and D.K. Edwards, AIChE J. 16 (1963) 594–601.

[16] D.D. Joseph, J. Fluid Mech. 47 (1971) 257–282.

[17] G.S. Charlson and R.L. Sani, Internat. J. Heat Mass Transfer 14 (1971) 2157–2160.

[18] J.C. Buell and I. Catton, Jour. Heat Transfer 105 (1983) 255–260.

[19] M.N. Sabry, Sur une nouvelle méthode intégrale et son application aux écoulements de fluides visqueux avec ou sans transfert de chaleurs, Thèse de Doctorat Es Sciences, Institut National Polytechnique de Grenoble. France, 1984.

[20] I. Mercader, M. Net and A. Falques, Comput. Methods Appl. Mech. and Engrg. 91 (1991) 1245–1251.

[21] D. Gottlieb and S.A. Orszag, Numerical Analysis of Spectral Methods: Theory and Applications (SIAM, Philadelphia, PA, 1977).

[22] J.P. Publicani, E. Crespo del Arco, A. Randriamampianina, P. Bountoux and R. Peyret, Internat. J. Numer. Methods Fluids 10 (1990) 481–517.

[23] C. Canuto, SIAM J. Numer. Anal. 23 (1986) 815–831.

[24] C. Canuto, M.Y. Hussaini, A. Quarteroni and T.A. Zhang, Spectral Methods in Fluid Dynamics (Springer, New York, 1988).

[25] M. Net, Convection in cylindrical geometry, Ph.D. Thesis, Barcelona University, 1991.

[26] D.L. Harris and W.H. Reid, Astrophys. J. Supp. Ser. 3 (1958) 429–447.

[27] S. Chandrasekhar, Hydrodynamic and Hydromagnetic Stability (Dover, New York, 1961).